

# Force network ensemble: a new approach to static granular matter

Jacco H. Snoeijer,<sup>1</sup> Thijs J. H. Vlugt,<sup>2</sup> Martin van Hecke,<sup>3</sup> and Wim van Saarloos<sup>1</sup>

<sup>1</sup>*Instituut-Lorentz, Universiteit Leiden, Postbus 9506, 2300 RA Leiden, The Netherlands*

<sup>2</sup>*Department of Physical Chemistry of Interfaces, Debye Institute, Utrecht University, Padualaan 8, 3584 CH Utrecht, The Netherlands*

<sup>3</sup>*Kamerlingh Onnes Lab, Universiteit Leiden, Postbus 9504, 2300 RA Leiden, The Netherlands*

(Dated: May 22, 2019)

An ensemble approach for force distributions in static granular packings is developed. This framework is based on the separation of packing and force scales, together with an a-priori flat measure in the force phase space under the constraints that the contact forces are repulsive and balance on every particle. We show how the formalism yields realistic results, both for disordered and regular “snooker ball” configurations, and obtain a shear-induced unjamming transition of the type proposed recently for athermal media.

PACS numbers: 45.70.-n, 45.70.Cc, 46.65.+g, 05.40.-a

The fascinating properties of static granular matter are closely related to the organization of the interparticle contact forces into highly heterogeneous force networks [1]. The probability density of contact forces,  $P(f)$ , has emerged as a key characterization of a wide range of thermal and athermal systems [2, 3, 4, 5, 6, 7]. Quite independently of the details of the interparticle potential or packing history,  $P(f)$  always has an exponential tail for large forces. Equally crucial is the generic change in qualitative behavior for small forces:  $P(f)$  exhibits a peak at some finite value of  $f$  for “jammed” systems which gives way to monotonic behavior above the glass transition [6, 7]. This hints at a possible connection between jamming and force network statistics and underscores the paramount importance of developing a theoretical framework for the force fluctuations and their spatial organization.

A first step towards a statistical description of force networks would be the definition of a suitable ensemble over which to take averages. A popular approach is that of Edwards, who proposed an equal probability for *all* “blocked” states of a given energy and density [8, 9]. However, averaging over this large space of packing configurations, with different packing topologies etc, is a hard problem. In (numerical) experiments, averages are simply taken over multiple realizations, but it is then difficult to properly sample a well-defined ensemble.

In this Letter we propose to avoid the complications associated with packing creation, by focussing immediately on the *ensemble of force configurations for a given fixed packing configuration* – see Fig. 1. The crucial ingredient is that in the limit in which the interparticle forces are harsh, *the spatial coordinates and interparticle forces become effectively decoupled*. As we will show, the forces are then underdetermined and the physics is dominated by the equations of force balance on each particle. Sampling all allowed configurations with equal probability then defines our ensemble. Even though our framework can easily be extended to 3D, we restrict ourselves

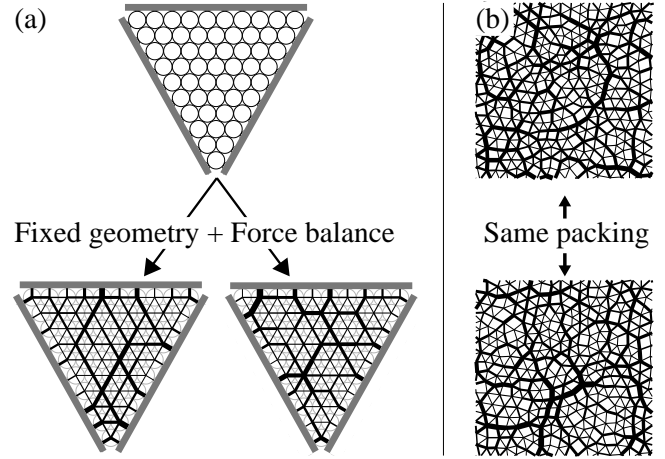


FIG. 1: Two different mechanically stable force configurations for (a) a “snooker-triangle packing” and for (b) an irregular contact network of 1024 particles (only part is shown); the thickness of the lines is proportional to the contact force. The “force network ensemble” samples all possible force configurations for a given contact network with an equal probability.

here to 2D packings of  $N$  frictionless disks of radii  $R_i$ , which have their centers at  $\mathbf{r}_i$ . We denote the interparticle force on particle  $i$  due to its contact with particle  $j$  by  $\mathbf{f}_{ij}$ . There are  $zN/2$  contact forces in such packings ( $z$  being the average contact number), and for purely repulsive central forces we can write  $\mathbf{f}_{ij} = f_{ij}\mathbf{r}_{ij}/|\mathbf{r}_{ij}|$ , where all  $f_{ij}$  are positive scalars. For a fixed contact topology, we are thus left with  $2N$  unknowns  $\mathbf{r}_i$  and  $zN/2$  unknowns  $f_{ij}$ . These satisfy the conditions of mechanical equilibrium,

$$2N \text{ eqs.: } \sum_j f_{ij} \frac{\mathbf{r}_{ij}}{|\mathbf{r}_{ij}|} = \mathbf{0}, \quad (1)$$

and once a force law  $F$  is given, the forces are explicit functions of the particle locations:

$$zN/2 \text{ eqs.: } f_{ij} = F(\mathbf{r}_{ij}; R_i, R_j). \quad (2)$$

For infinitely hard particles, Eqs. (2) reduce to  $zN/2$  constraints on the  $2N$  coordinates  $\mathbf{r}_i$ , and these can only be satisfied if  $z \leq 4$ . Since on the other hand Eqs. (1) can only be solved if  $z \geq 4$ , packings of infinitely hard particles have to be *isostatic* so that  $z = 4$ ; in  $d$  dimensions this “critical” value becomes  $z = 2d$ . [10, 11].

However, for realistic particles of finite hardness, packings are typically *hyperstatic* with  $z > 2d$ . A key parameter is  $\varepsilon \equiv (\bar{f}/R)(dr_{ij}/dF)$ , and in simulations of 3D particles for which  $\varepsilon \sim 10^{-3}$ ,  $z$  is still 6.4 [12]. We avoid the strict  $\varepsilon \downarrow 0$  limit, but we keep in mind that typical changes in the contact forces result in minute particle deformations only. For  $\varepsilon \ll 1$  we therefore expect the force balance constraints Eqs. (1) to dominate and we consider  $\mathbf{r}_i$  as fixed. In this case there are more degrees of freedom ( $zN/2$ ) than constraints ( $2N$ ), leading to many possible force configurations that obey mechanical equilibrium - see Fig. 1. Our main idea is to explicitly separate contact and force geometry, and to restrict ourselves to the *ensemble of force networks* for a *fixed* contact geometry.

It is important to note that different points in our ensemble do not correspond to physical realizations of the *same* set of particles with a *given* force law. However, the overall properties of granular packings do not depend strongly on details of the force law or particle shape [5, 6]. Our ensemble can, e.g., be interpreted as sampling realizations with slightly varying force laws. Alternatively, we can consider particles which are not perfectly round - think of a “regular” packing of real cannon balls [13].

The ensemble of force networks for a fixed contact geometry is constructed as follows. (i) We start from an a-priori flat measure in the force phase space  $\{f\}$ . (ii) We impose the  $2N$  *linear* constraints given by the mechanical equilibrium Eqs. (1). (iii) We furthermore consider repulsive forces only, i.e.,  $\forall f_{ij} \geq 0$ . (iv) We set an overall force scale by applying a *fixed pressure*, similar to implementing proper constraints of fixed energy or particle number in the usual thermodynamic ensembles.

Below, we will first illustrate our formalism for a regular “snooker” packing (Fig. 1a). Then, for an irregular packing of 1024 particles (Fig. 1b), we investigate the role of the “hardness”  $\varepsilon$  and find that applying a shear stress yields an “unjamming” transition. Our approach captures the essential features of the force networks of hard particles, leads to new insights on both the universal tail and non-universal “shoulder” of  $P(f)$  and is conceptually simple and numerically cheap.

*Regular packings* The snooker-triangular packings shown in Fig. 1a have  $z = 6$ , and therefore have  $3N$  unknown forces that are constrained by the  $2N$  equations of mechanical equilibrium. Labeling each bond by a single index  $k$ , the mechanical equilibrium can be expressed as

$$A\vec{f} = \vec{0} \quad \text{with} \quad \vec{f} \equiv (f_1, f_2, \dots, f_{3N}), \quad (3)$$

where  $A$  is a  $3N$  times  $2N$  sparse matrix. There is thus an  $N$ -dimensional subspace of allowed force configura-

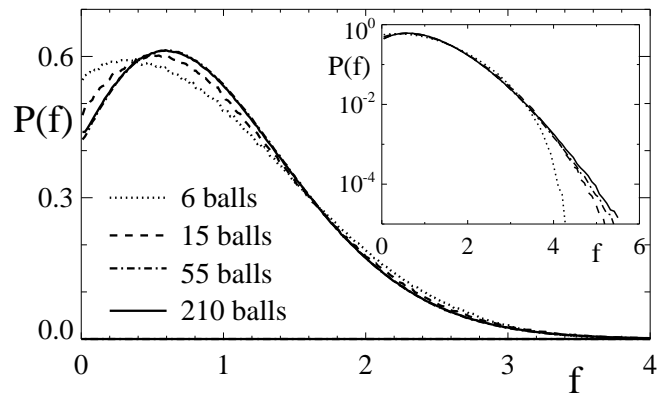


FIG. 2:  $P(f)$  for various “snooker” packings, with the inset showing the emergence of an exponential tail for large systems.

tions that obey mechanical equilibrium. Eq. (3) is homogeneous, but in physical realizations an overall force scale is determined by the externally applied stresses and/or the gravitational bulk forces. The simplest manner to do so here is to fix the external pressure by specifying the total boundary forces. For the snooker-triangles it then follows that the sum of all forces is constant:

$$\sum_k f_k = F_{\text{tot}} = zN/2 \bar{f}. \quad (4)$$

We will show below, using the microscopic expression for the stress tensor, that this constraint also holds for irregular packings.

We are thus considering the phase space defined by the force balance (3), the overall force constraint (4), and the condition that all  $f$ ’s are positive:

$$\mathcal{A}\vec{f} = \vec{b} \quad \text{and} \quad \forall f_k \geq 0, \quad (5)$$

where the fixed matrix  $\mathcal{A}$  is the matrix  $A$  extended by the stress constraint and  $\vec{b} = (0, 0, 0, \dots, 0, F_{\text{tot}})$ .

To compute  $P(f)$  for larger packings, we have applied a simulated annealing procedure [14]. Starting from an ensemble of random initial force configurations we sample the space of mechanically stable networks, using a penalty function whose degenerate ground states are solutions of Eq. (5). We have carefully checked that results do not depend on the initial configurations, and furthermore perfectly reproduce the 3 and 6 balls cases, where we can work out  $P(f)$  (semi)analytically [15].

The two force networks shown in Fig. 1 are typical solutions  $\vec{f}$  obtained by this procedure. The resulting force distributions for packings of increasing number of balls are presented in Fig. 2. Note that all  $P(f)$ ’s display a peak for small  $f$ , which is typical for jammed systems [6]. For large packings, this peak rapidly converges to its asymptotic limit, and we recover the exponential tail for large forces as well (see inset Fig. 2).

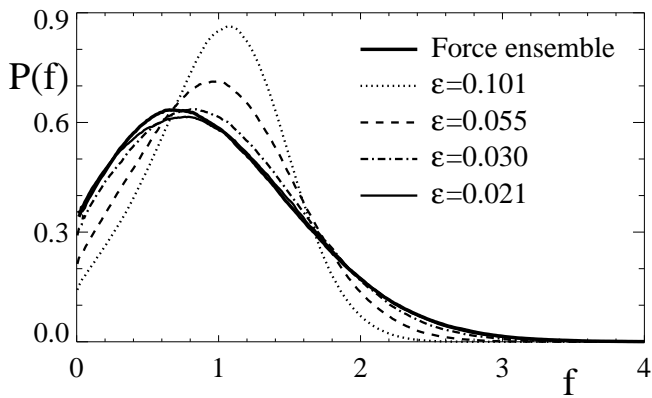


FIG. 3: Comparison of the  $P(f)$  obtained by our sampling of a frozen geometry, and MD simulations of increasingly hard particles under constant pressure in the limit  $T \rightarrow 0$ .

The realistic force networks and  $P(f)$ 's thus obtained illustrate the validity of our approach, and allow us to speculate about the origin of the shape of  $P(f)$  within the context of our formalism. When we ignore the mechanical equilibrium Eq. (3) and only combine the normalization constraint Eq. (4) with the requirement of positivity,  $P(f)$  becomes a pure exponential, by the same mechanism through which the Boltzmann distribution of energies  $E_i$  of subsystems arises from the microcanonical ensemble. Once the mechanical equilibrium constraints are added, deviations from purely exponential behavior occur for small forces, but the “normalization constraint” remains apparently dominant for large forces, thus yielding an exponential tail but a non-universal shoulder.

*Irregular packings* We now apply our force ensemble approach to a more realistic system with a random packing geometry, and study a shear-stress induced unjamming transition. To obtain a representative irregular contact geometry, we perform a standard Molecular Dynamics simulation of 1024 bidisperse particles (size ratio 1.4) that have a purely repulsive 12-6 Lennard-Jones interaction (a shifted potential with the attractive tail cut off), the same system as the one studied by O’Hern *et al.* [6]. We then quench such a finite temperature simulation onto a  $T = 0$  random packing with a steepest descent algorithm [14]. The static contact network that we obtain in this way then defines the matrix  $\mathcal{A}$  in Eq. (3).

The  $P(f)$  obtained by the force ensemble approach for this fixed packing is displayed in Fig. 3: even for a single contact geometry, we clearly reproduce a realistic  $P(f)$  which is very similar to both that of the triangular packings and to those obtained in experiments and simulations [2, 5].

To investigate the role of the particle hardness, we have performed MD simulations of the same system with increasingly hard particles. For our original MD, which defined  $\mathcal{A}$ , the particles are of intermediate hardness with  $\varepsilon \sim 0.1$ , and the corresponding  $P(f)$  is somewhat dif-

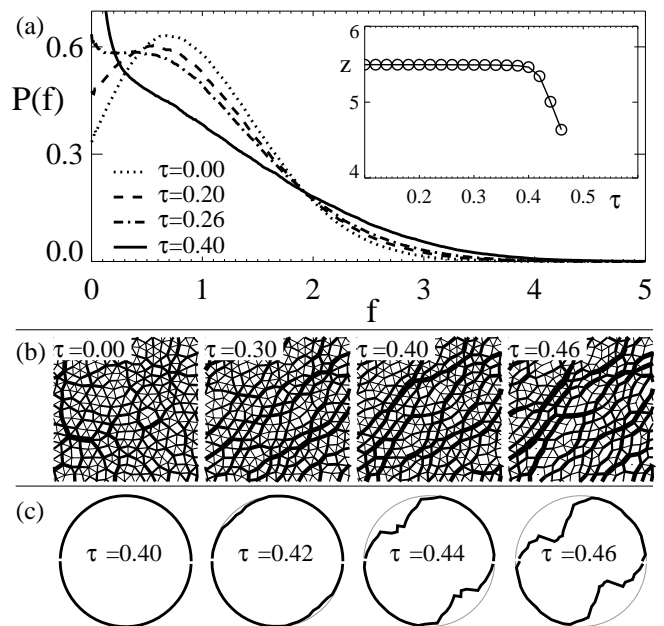


FIG. 4: Force networks under shear. (a)  $P(f)$  for increasing shear showing an “unjammed” transition at  $\tau \approx 0.26$ . The inset shows the contact number as function of shear, where contacts are considered broken when  $f < 10^{-4}$ ; for smaller values of the cutoff this curve remains essentially the same. (b) Examples of parts of the force networks under shear (c) Ratio of number of contacts with  $f > 10^{-4}$  and number of contacts as function of the contact angle show preferential breaking along the “weak” principal direction.

ferent from the one in the force ensemble. When the hardness of the particles is increased,  $\varepsilon$  diminishes and the corresponding  $P(f)$  indeed approaches the force ensemble  $P(f)$ . For the hardest particles ( $\varepsilon \sim 0.02$ ) these  $P(f)$ 's are virtually indistinguishable. We find that this holds for a variety of force laws [15]. This confirms the validity of our approach for hard particles.

*Unjamming by shear* It is also possible to study the effect of a shear stress on the force network ensemble by using the relation between the microscopic forces and the macroscopic stress field:

$$\sigma_{\alpha\beta} = \frac{1}{V} \sum_k (\mathbf{f}_k)_\alpha (\mathbf{r}_k)_\beta, \quad (6)$$

and extending the matrix of Eq. (5) with the three *linear* constraints of Eq. (6). Note that  $|\mathbf{r}_k|$  is essentially the average diameter of the two hard particles in contact, so that setting the trace of  $\sigma$  (i.e. the pressure) equal to unity does indeed lead to a constraint of the form Eq. (4) [16]. The average value of the force is set to unity by requiring  $\sigma_{xx} = \sigma_{yy} = 1/2$ , and we vary  $\tau = \sigma_{xy}/\sigma_{xx}$ .

We find that  $P(f)$  evolves from a “jammed” distribution with a peak, to an “unjammed” monotonous distribution as a function of shear stress (Fig. 4a). As function of the angle  $\phi$ ,  $\langle f \rangle$  varies in good approximation as

$1+2\tau\sin(2\phi)$ . This variation is consistent with Eq. (6) as well as with the alignment of the dominant contacts visible in Fig. 4b – note the similarity to experimentally obtained sheared networks [17]. Since  $P(f)$  contains forces in all directions, the broadening of  $P(f)$  with shear stress follows immediately from this angular modulation of  $\langle f \rangle$ . However, this is only part of the story: we find that the *shape* of  $P(f)$  also varies with direction, from extremely jammed along the force lines, to almost purely exponential along the weak principle direction (not shown) [15].

When  $\tau$  approaches  $1/2$ ,  $\langle f \rangle$  becomes zero along the weak principle direction, which implies that all forces along the weak direction approach zero. This can be interpreted as the breaking of contacts (see Fig. 4c). In addition, when  $\tau \rightarrow 1/2$ , the contact number drops to  $z = 4$  (inset of Fig. 4a), and beyond this point, stable force networks are no longer possible. This simple mechanism thus provides  $\tau = 1/2$  as a definite upper bound for the critical yield stress, a phenomenon that is not well understood theoretically [1, 13, 18, 19]. In terms of the “slip angle” this value corresponds to an angle of  $30^\circ$ . On the other hand, it has been speculated [6, 7] that the qualitative change of  $P(f)$  from peak to plateau could also be indicative of yielding; in our ensemble this occurs at  $\tau = 0.26$  suggesting a slip angle of  $15^\circ$ .

*Outlook* We have proposed a novel approach to static granular matter, based on fixed hyperstatic packings of hard particles. No further approximations were made, and the full set of mechanical equilibrium constraints were incorporated, this in contrast to more local approximations [3, 4, 20, 21] or force chain models [22]. A number of crucial questions can possibly be addressed within our framework. (1) Friction is difficult to express in a force law similar to Eqs. (2) but simple to think about in terms of the Coulomb inequality. Our framework is thus perfectly suited to include frictional forces. It should be noted that frictional packings are strongly hyperstatic and underdetermined, even for infinitely hard particles [12]. (2) Sand piles under different construction histories exhibit a varying level of anisotropy in their contact and force networks [23, 24]. One way of thinking suggests that the forces are “frozen in” during preparation, but we suggest that, in our ensemble approach, contact network anisotropies may be sufficient to obtain the pressure dip under properly created piles. (3) The extension of our framework to nonzero temperatures is nontrivial, but work in progress indicates that upon allowing the zero elements of the vector  $\vec{b}$  in Eq. (5) to become nonzero with mean square average proportional to  $T$  captures the essential temperature behavior as well. Interestingly, for temperature induced unjamming, the force lines become shorter and of less importance [6], while for shear induced unjamming, the force lines become increasingly pronounced. (4) The problem defined by Eqs. (5) could be generalized by no longer associating the matrix  $A$  with a packing. In its most general form, for arbitrary  $\mathcal{A}$  and

$\vec{b}$ , we can calculate  $P(f)$  and may ask under what conditions  $P(f)$  has an exponential tail, appear jammed or unjammed etc. Some preliminary data suggests that already for small random matrices one obtains a  $P(f)$  with a peak at small  $f$ , while even for large random matrices  $P(f)$  appears to have a Gaussian tail. Presumably, local interactions (i.e., a *sparse* matrix  $\mathcal{A}$ ) are crucial to obtain an exponential tail for  $P(f)$ .

We are grateful to Jan van der Eerden, Alexander Morozov and Hans van Leeuwen for numerous illuminating discussions. JHS gratefully acknowledges support from the physics foundation FOM, and MvH support from the science foundation NWO through a VIDI grant.

- 
- [1] H. M. Jaeger *et al.*, Rev. Mod. Phys. **68**, 1259 (1996); P. G. de Gennes, Rev. Mod. Phys. **71**, 374 (1999).
  - [2] D. M. Mueth *et al.*, Phys. Rev. E **57**, 3164 (1998); D. L. Blair *et al.*, Phys. Rev. E **63**, 041304 (2001); G. Løvoll *et al.*, Phys. Rev. E **60**, 5872 (1999).
  - [3] J. Brujic *et al.*, Faraday Discussions **123**, 207 (2003).
  - [4] S. N. Coppersmith *et al.*, Phys. Rev. E **53**, 4673 (1996).
  - [5] F. Radjai *et al.*, Phys. Rev. Lett. **77**, 274 (1996); S. Luding, Phys. Rev. E **55**, 4720 (1997); F. Radjai *et al.*, Phys. Rev. Lett. **80**, 61 (1998); A. V. Tkachenko and T. A. Witten, Phys. Rev. E **62**, 2510 (2000); S. J. Antony, Phys. Rev. E **63**, 011302 (2000); C. S. O’Hern *et al.*, Phys. Rev. Lett. **88**, 075507 (2002).
  - [6] C. S. O’Hern *et al.*, Phys. Rev. Lett. **86**, 111 (2001).
  - [7] L. E. Silbert *et al.*, Phys. Rev. E **65**, 051307 (2002).
  - [8] S. F. Edwards and R. B. S. Oakeshott, Physica A **157**, 1080 (1989).
  - [9] H. A. Makse and J. Kurchan, Nature **415**, 614 (2002).
  - [10] C. F. Moukarzel, Phys. Rev. Lett. **81**, 1634 (1998).
  - [11] A. V. Tkachenko and T. A. Witten, Phys. Rev. E **60**, 687 (1999).
  - [12] L. E. Silbert *et al.*, Phys. Rev. E **65**, 031304 (2002).
  - [13] J. Duran, *Sand, powders and grains*, Springer-Verlag, New York 2002.
  - [14] W. H. Press *et al.* *Numerical Recipes: The Art of scientific computing*, (Cambridge University Press, Cambridge, England 1986).
  - [15] J. H. Snoeijer *et al.*, in preparation.
  - [16] We take  $r_k$  out of the sum which again is allowed in the hard particle limit and at high pressures.
  - [17] J. Geng *et al.*, cond-mat/0211031.
  - [18] R. M. Nedderman *Statics and Kinematics of Granular Materials*, (Cambridge University Press, Cambridge, England 1992).
  - [19] J. Lee and H. J. Herrmann, J. Phys. A **26**, 273 (1993); R. Albert *et al.*, Phys. Rev. E **56**, R6271 (1997); A. Daerr and S. Douady, Nature **399**, 241 (1999).
  - [20] K. Bagi, Granular Matter **5**, 45 (2003).
  - [21] T. C. Halsey and D. Ertas, Phys. Rev. Lett. **83**, 5007 (1999).
  - [22] J. P. Bouchaud *et al.* Eur. Phys. J. E **4**, 451 (2001).
  - [23] L. Vanel *et al.*, Phys. Rev. E **60**, R5040 (1999).
  - [24] J. Geng *et al.*, Phys. Rev. E **64**, 060301 (2001).